A Discussion of the Application of the Migration Process to Western Geophysical Company Seismic Reflection Line W74-12 in the Vicinity of the Hosgri Fault Zone, in the Area Offshore from the Diablo Canyon Power Plant Site

Introduction

The basic concepts of "Common Depth Point" (CDP) seismic reflection data acquisition, "velocity analysis", and the transformation of seismic data from a time-distance domain to a distance-distance domain will be discussed in this report. These concepts will facilitate a detailed discussion of observed seismic reflection velocities and the effects of velocity variations on the apparent location of geologic structures associated with the Hosgri fault zone adjacent to the Diablo Canyon nuclear reactor site. Reflectors observed on seismic section W74-12 will be used as examples to quantitatively show the errors in reflector positioning resulting from geologically reasonable variations of RMS velocity values extant in this area.

Common Depth Point Processing

The techniques used by Western Geophysical Company to determine offshore subsurface velocities are an integral part of the Common Depth Point (CDP) stacking procedure used to improve the signal-to-noise ratio of seismic reflection data. The CDP process was first introduced by Mayne in 1962. The technique improved S/N ratios by signal averaging, but did not lower the resolution of the seismic data (a problem intrinsic to all previous signal averaging methods). The CDP method utilizes a geometry of shot points and receiver positions such that a single reflection point may be recorded along several different ray paths (see Figure 1). The seismic traces recording a common depth point are moved along a vertical time axis until identical reflection points are aligned. The traces are then summed ("stacked"). Ideally, the reflectors add constructively, and random perturbations sum to a low average valve. The net signal enhancement is equal to the square root of the number of traces summed (Mayne, 1962).

Velocity Analysis

Accurate velocity data are crucial in normalizing CDP travel times to provide proper reflector alignment before stacking. Figure 2 shows how a high frequency signal can be degraded by stacking with time misalignments as small as 4 milliseconds (Dee,

1975). CDP "gathers" are constructed to facilitate the accurate determination of velocities. A "gather" is a panel of all the traces from the same common depth point arranged with the shot times (t = 0) forming a horizontal line (Figure 3). CDP traces gathered and arrayed in order of increasing distance from the energy source will show a common reflection point as a hyperbola. The hyperbola characteristic of each reflection point can be fitted by the equation (Cook and Taner, 1968):

$$T_x^2 = T_o^2 + \frac{X^2}{\overline{V}^2}$$

Where T_x = the travel time to the reflector

T_o = the normal incidence travel time

X = the distance from the trace to the energy source

$\overline{V}$ = the RMS velocity to the reflector.

Thus, it can be seen that the curve fitting process will yield a unique $\overline{V}$ to each reflector beneath the common depth point.

Hyperbolae formed by near surface reflectors will have more curvature than those formed by relatively deep reflectors. Hyperbolae with pronounced curvatures can be more accurately fitted by a mathematical equation than can those with small curvatures. The amount of hyperbolic curvature displayed on a "gather" panel will also depend on the length of the geophone spread; the larger the spread, the larger the amount of the curvature displayed. Hence, the depth to which a velocity analysis is reliable is directly proportional to the spread length.

Velocity Spectral Analysis

A "Velocity Spectrum" may be constructed from a number of velocity analyses. Such a spectrum may be used to determine $\overline{V}$ and the relative reliability of $\overline{V}$ throughout a time-distance domain seismic record section. Cook and Taner (1969) concisely describe the procedures used to construct a Velocity Spectrum.

> "Velocity Spectral analysis computes and displays the coherent power among a set of common depth point traces (CDP gather) according to various hyperbolic curves as given by the equation $T_x^2 = T_o^2 + \frac{X^2}{\overline{V}^2}$. A Velocity Spectrum is computed at a given normal incidence time by hyperbolic searches covering a gate of 50 milliseconds made in velocity increments of 100 feet per second. This is then repeated down the

record at 24 millisecond intervals. The amplitude of the resulting trace, which is indicative of the coherent power in the spectrum, is measured by a multi-channel filter such as is schematically shown in Figure 4. This figure shows three hyperbolic curves and their corresponding power on the spectrum.

Figure 3 shows an actual example taken from the Gulf of Mexico in an area where reflections are plentiful and mostly primaries."

Velocity Spectra may be degraded by a number of factors. The lack of coherent reflectors or acoustic anisotropies which disrupt the signals to distant geophones will render the Velocity Spectrum unusable. Diffracted seismic returns and intra-bed multiple reverberations will cause multiple spectral peaks and/or a broadening and reduction of the power within a spectral peak. Dipping beds will cause the Velocity Spectrum to indicate anomalously high velocities.

Time-Distance to Distance-Distance Transformation

The position of a reflecting bed in a time-distance domain will be different from that of the reflector in a distance-distance domain. The basic reason for this is illustrated in Figure 5. More complete discussions of the transformation from one domain to the other are given by Slotnick (1959) and Gates (1957). The term generally applied to the transformation process is migration.

Slotnick (1957, p 63-68) outlines a simple geometric procedure for migration. The process involves calculating the true dip of the center of the reflector from the formula:

$$\sin\alpha = \Delta t / \Delta x$$

Where α = the dip of the reflector

Δt = the travel time difference from one end of the reflector to the other

Δx = the horizontal distance spanned by the reflector on the time-distance record section.

The true position of the center of the reflector will then lie along the radial $\overline{SS'}$ as shown on Figure 5. The distance $\overline{SO}$ will depend upon the RMS velocity ($\overline{V}$) determined

for that reflector from a Velocity Spectral analysis.

Using Slotnick's migration technique, it can be seen that the position of a migrated reflector changes as $\overline{V}$ is varied. The position change will be a function of $\overline{V}$ and α or

$$\Delta H\,(\overline{V},\alpha) = (\Delta V)\,\frac{t}{2}\,\sin\alpha$$

Where ΔH is the horizontal change in position of a reflector, ΔV is the change in $\overline{V}$, and t is the two-way travel time to the center of the reflector.

From this equation, it can be seen that increasing $\overline{V}$, t, or α will increase displacement of the reflector from its unmigrated position. Thus, in geologic terms, the higher the rock velocities, the deeper the reflector and the greater its dip, the greater the change in the reflector position as a result of the migration process.

Interpretation of Seismic Profile W74-12

Reliability of Velocity Data

The field procedures used in shooting Line W74-12 provided a 46 fold multiplicity of common depth points. Hence, the large geophone spreads used to make the CDP gathers from which the Velocity Spectra shown in Plate II* are obtained cover widely divergent ray paths. This imparts a high sensitivity to the Velocity Spectra. In general, the field and processing procedures used by Western in deriving their velocity data are such that the data are of the highest quality obtainable with present production technologies.

It is possible to obtain approximate error limits for the velocities used to migrate Line W74-12. This may be done by re-interpreting the velocity spectra for this line and by comparing the values derived from the Western data with velocity data obtained from Aquatronics Line PB-4. This line is parallel to and 0.5 miles south of Line W74-12. Plate I* shows the Velocity Spectra for Line W74-12, and Table I* shows the actual velocity functions used by Western to migrate Line W74-12. These velocity functions have been drawn on Velocity Spectra 268 and 220 of Plate I.* These are the two analyses nearest to the Hosgri fault zone. Also drawn on the Velocity Spectra are Earth Sciences Associates (ESA) re-interpretations of the Western velocity functions.

(*) Proprietary data, not included with this report copy.

The ESA velocity functions indicate lower velocities than those used by Western, but nowhere do the ESA values deviate by more than -10% from the Western values.

Spectrum 268 is ambiguous in the time interval between 0.4 and 0.8 seconds. The first small peak of the broad double peak in this region is interpreted as a multiple reflection. The Western velocity values definitely appear to be about 8% too high in this region. In the time interval from 0.8 to 1.6 seconds, the $\overline{V}$ values are well defined. The precursory peaks in the interval from 1.1 to 1.2 seconds are probably caused by multiple reverberations associated with the reflectors in the 0.8 second range. The broad trailing peaks in the 1.2 to 1.4 second interval are inferred to originate from diffracted energy associated with the buried reverse fault west of the Hosgri fault. Below 1.6 seconds, the quality of the velocity spectrum diminishes as the reflectors in this time interval display less coherency than the reflectors in the overlying strata. Below 2.0 seconds (the region of the Acoustic Unit A-2, A-3 interface), no useful velocity data are observed.

Velocity Spectrum 220 displays are of lower quality than those of Spectrum 268. Below 0.5 seconds, the peaks are very broad, possibly a result of multiple reflections and spurious diffracted energy associated with the Hosgri fault. The ESA interpretation considers velocities below 0.5 seconds to be of low reliability and data below 0.7 seconds not to be useful.

Velocity data produced by Aquatronics, Inc. for the processing of Line PB-4 show substantially higher velocities than are obtained from the Western data. The velocity functions used by Aquatronics are shown in Figure 6. The functions labeled NMO 580 and NMO 291 approximately correspond to Western Velocity Spectral analyses 220 and 268, respectively. In comparing NMO 291 with Western Spectrum 268, the Aquatronics velocity is found to be at most 37% higher than the Western values at the 1.0 second time mark. Comparison of NMO 580 with Spectrum 220 indicates a maximum discrepancy of 21% which is reached at the 0.5 second mark, the point below which lack of reflector coherency is inferred to render both Western and Aquatronics data unusable.

The intrinsic reliability of the Aquatronics velocity data is lower than that of the Western data. The data collection procedures used by Aquatronics are directed toward the acquisition of shallow penetration, high resolution data. As a consequence, they cannot utilize the long geophone spreads necessary to obtain large CDP multiplicity. The Aqua-

tronics data are 6 fold stacks. Therefore, the divergence of ray paths used to compute their Velocity Spectra are much less than those used by Western. The reliability of the Aquatronics velocity data is correspondingly diminished, particularly at deeper penetrations.

In summary, by comparing Aquatronics velocity data to Western velocity data, an upper bound of velocity error may be postulated, and by re-interpreting Western data, a lower bound may be established. The Aquatronics data set an upper error boundary of +37%. Re-interpretation of the Western data sets a lower error boundary of -10%. The reliability of the Western velocity values used to migrate Line W74-12 is thus postulated to be +37% and -10%.

Effects of Velocity Variation on the Migrated Location of a Reflector

The following discussion illustrates the effects of velocity errors on the migration of reflectors within the Hosgri fault zone. Additionally, the discussion shows quantitatively the effects of the velocity errors on two hypothetical faults, one of which is coincident with the Hosgri fault.

The locations of both the buried reverse fault west of the Hosgri fault and the Hosgri fault itself have been accurately plotted directly from the time-distance record section of Line W74-12. These faults have been located by plotting the crests of diffraction cones formed when acoustic energy is inferred to be diffracted from the terminations of beds against the fault plane. The crests of the diffraction hyperbolae mark the position of the bed terminations, which act as point diffraction sources, in their proper lateral position on the time-distance plot (Tucker and Yorjston, 1973). Thus, the locations of both the buried reverse fault, and the part of the Hosgri fault below 0.5 seconds, are mapped on Line 74-12 by a method that is not subject to the velocity-dependent position errors that affect structures which must be mapped on the basis of reflector positions. The uppermost part of the Hosgri fault has been located in the same manner on high resolution seismic lines adjacent to and coincident with Line W74-12.

The following values and methods were used to evaluate the migration effects of velocity errors. As previously stated, the velocity errors were considered to be -10% and +37% of the values used by Western Geophysical Company to migrate Line W74-12.

The algorithm used to migrate the reflectors is as outlined by Slotnick (1959).

The shift in position of a reflector resulting from the migration process increases with the depth of the reflector. Three deep reflectors were migrated using the nominal, and maximum and minimum expected velocities. The results of the analysis are shown in Figure 7. Clearly, as expected, the deepest reflector, Number 3 has the widest range of positions. If the $\bar{V}$ value used was 37% higher than the nominal value, then the center point of the reflector would change about 3500 feet horizontally and 2200 feet vertically from its unmigrated position. Also, notice that on Plate I* the eastern termination of Reflector 3 appears to be related to the buried reverse fault. After migration, it can be seen that this cannot be the case, as the actual spatial location of Reflector 3 is over a mile west of the fault. This example shows the importance of considering the effects of migration when viewing time-space domain record sections.

If the buried reverse fault west of the Hosgri fault was located on the basis of the position of adjacent reflectors, its position would change as shown in Figure 6. The exact numeric value of the change in spatial location of the fault depends strongly on the location of the reflectors used to demark it, and on the assumed direction of inclination of the fault. However, in general, lowering velocities will move a fault of this orientation shoreward, and raising velocities will move it seaward relative to its unmigrated position. Again, it is to be stressed that the actual position of this fault as plotted on Plate I* is not affected by the migration errors. The example is used to give a quantitative picture of the magnitude of the general problem of migration errors in the vicinity of the Hosgri fault.

The effects of velocity errors on the migrated positions of structures diminishes as the depth of the structure decreases. This is illustrated by the small change in the position of the Hosgri fault shown in Figure 8. The total change in surface position of the Hosgri fault ranges only over 100 feet. This small error range is due in part to the nearly vertical orientation of the Hosgri fault. If the structure had a greater dip, increases in velocity values would tend to migrate the fault seaward, and velocity decreases would relocate the fault shoreward. Even if reflector dips were raised to 30° (the range of the steepest dips that can be recorded by the seismic reflection technique), the displacement of the fault structure would not exceed 500 feet. Thus, provided the structures of interest are shallower than about 1500 feet, position errors associated

(*) Proprietary data, not included with this report copy.

with velocity (migration) errors are relatively small.

It is again stressed that the Hosgri fault in the vicinity of Line W74-12 is positioned on the basis of diffraction cones. But, even if its position was determined by the positioning of adjacent reflectors, its near-surface location would not vary at the most by more than 500 feet and probably not more than 100 feet from its presently plotted surface location.

References Cited

Cook, E. E., and M. T. Taner (1969). Velocity Spectra and Their Use in Stratigraphic and Lithologic Differentiation. Geophys. Prospecting, vol. 17, no. 4, p 433-448.

Dee, M. (1975). Digital CDP Procedures Provide New Capability for High Resolution Seismic Data. Paper presented at the Seventh Annual Offshore Technology Conference, Houston, Texas, May 5-8.

Gates, J. P., 1957. Descriptive Geometry and the Offset Seismic Profile. Geophysics, vol. 22, no. 3, p 589-609.

Mayne, W. H. (1962). Common Reflection Point Horizontal Data Stacking Techniques. Geophysics, vol. 27, no. 6, p 927-938.

Slotnick, M. M. (1959). Lessons in Seismic Computing. Pub. Society of Exploration Geophysicists, 268 p.

Tucker, P. H., and H. V. Yorjston (1973). Pitfalls in Seismic Interpretation. Soc. Exploration Geophysicists Monograph Series, no. 2, 50 p.

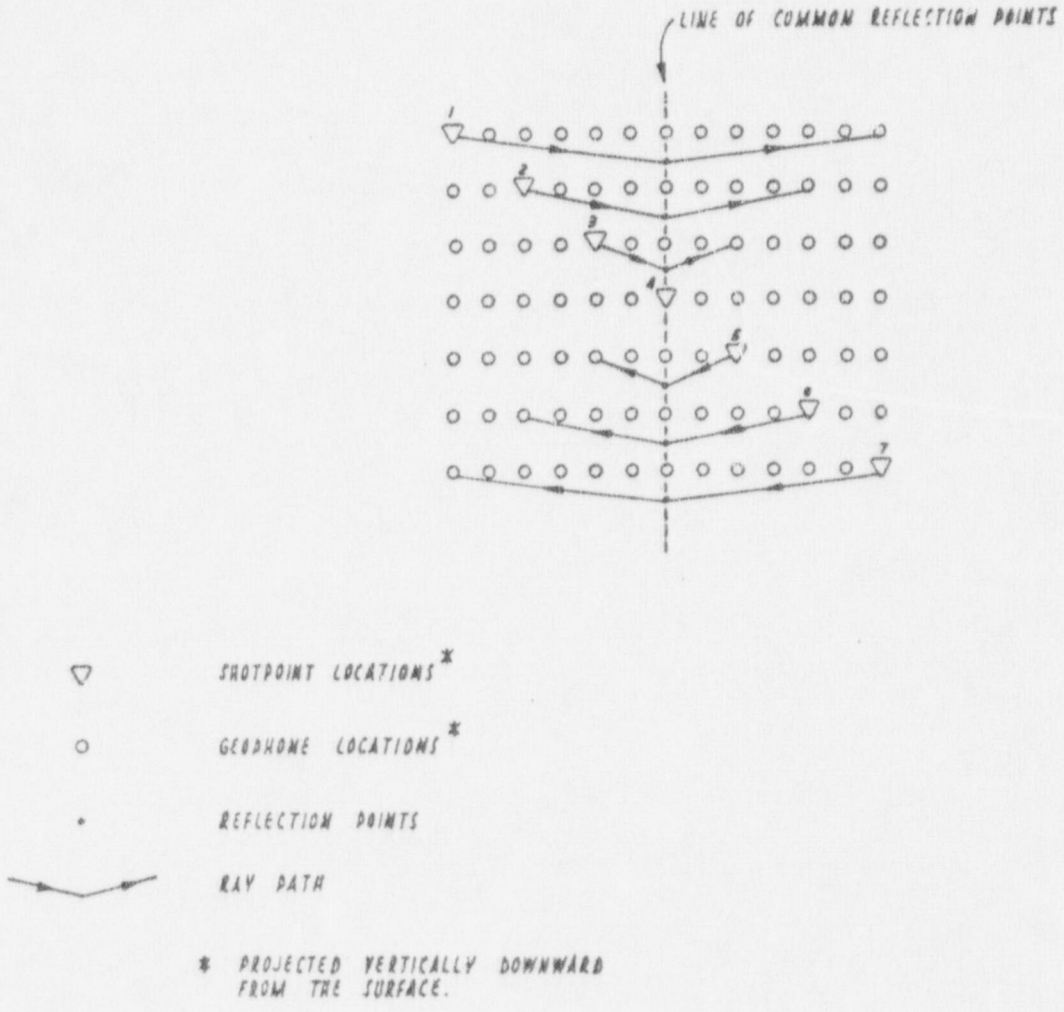

Figure 1. This diagram shows CDP geophone-shotpoint geometry giving a six fold multiplicity for each reflection occurring beneath the dashed line labeled "Line of common reflection points". A spot on each reflector located directly below the common depth point (or line of common reflectors) will be recorded on six different seismic traces by waves traversing different ray paths.

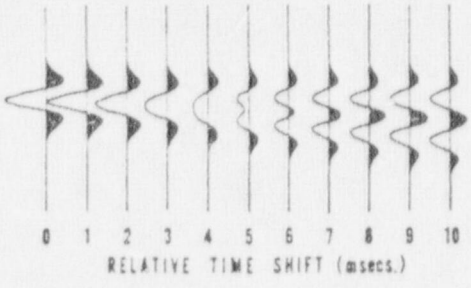

Figure 2. Two-wavelet summation model using perfect 100 Hz Ricker wavelets. This model illustrates the degradation of a stacked signal resulting from improper pre-stack time alignment.

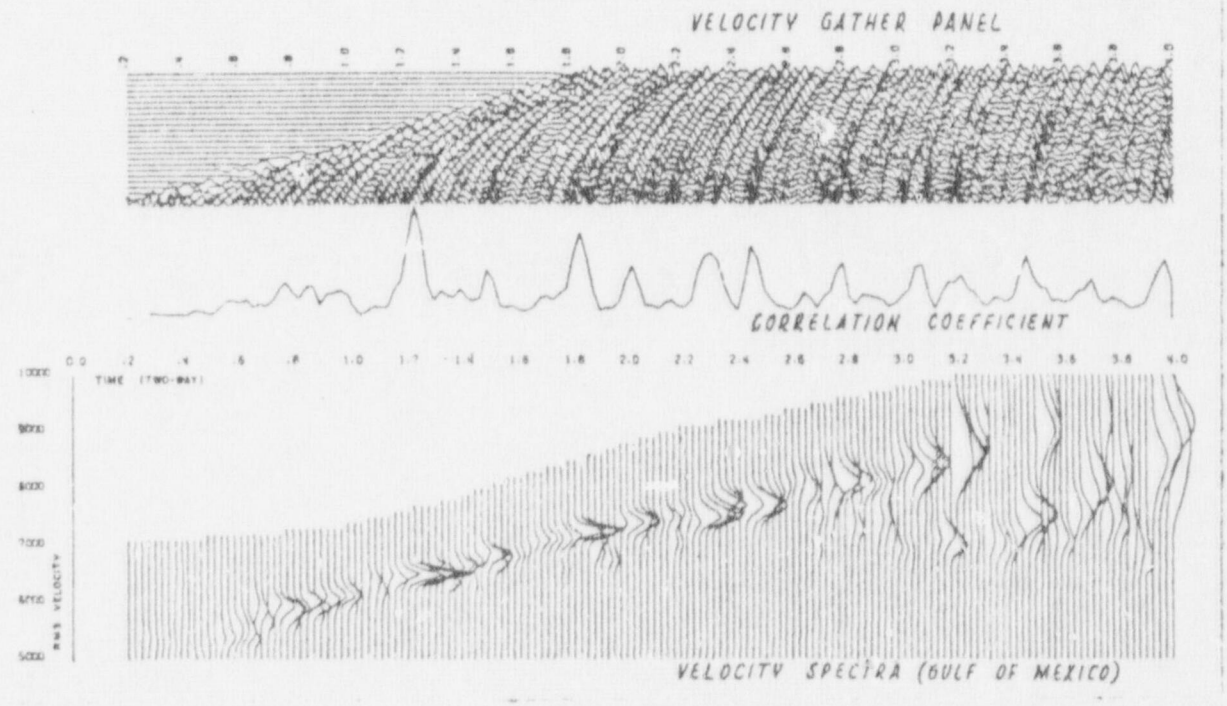

Figure 3. Typical Velocity Spectra Display in a Good Reflection Area (Cook and Taner, 1968).

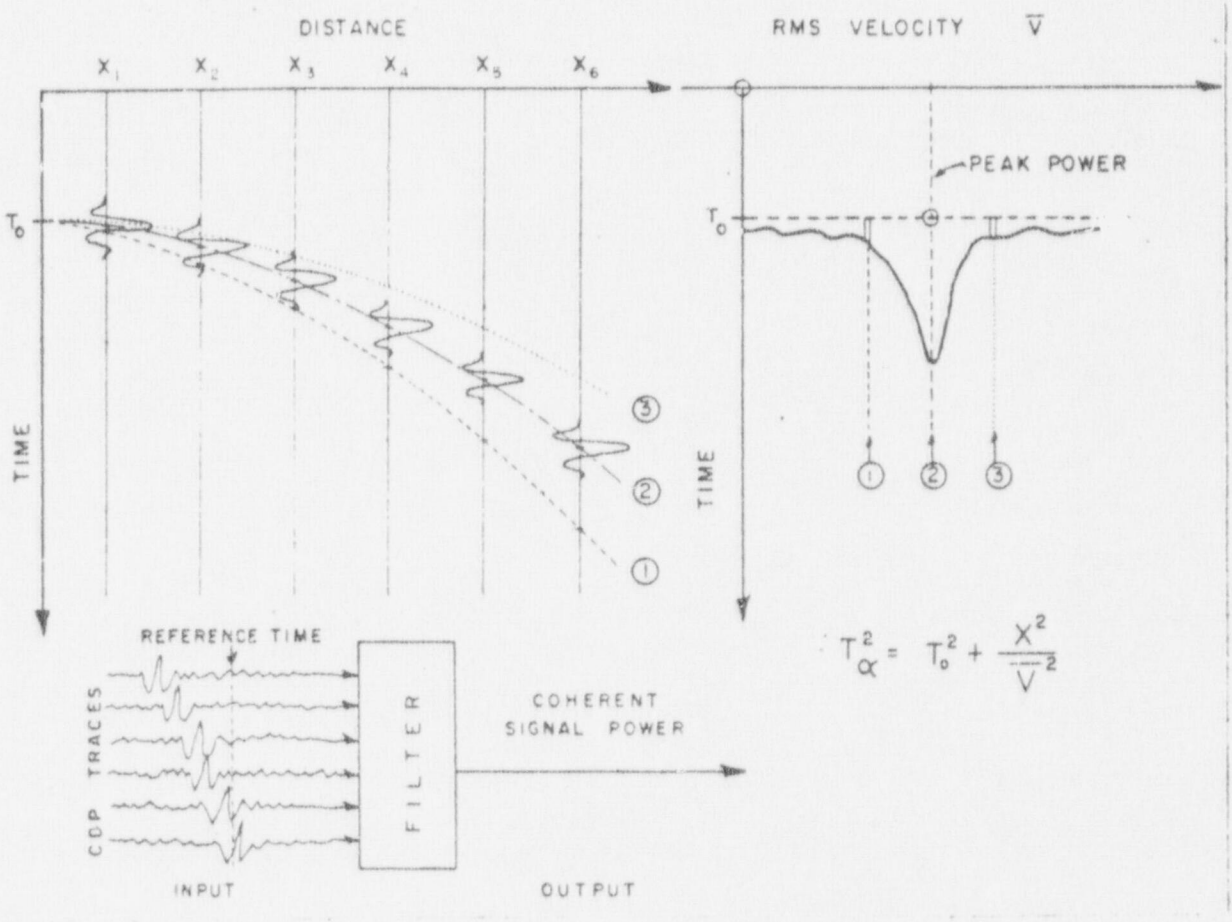

Figure 4. Derivation of a Velocity Spectrum (Cook and Taner, 1968).

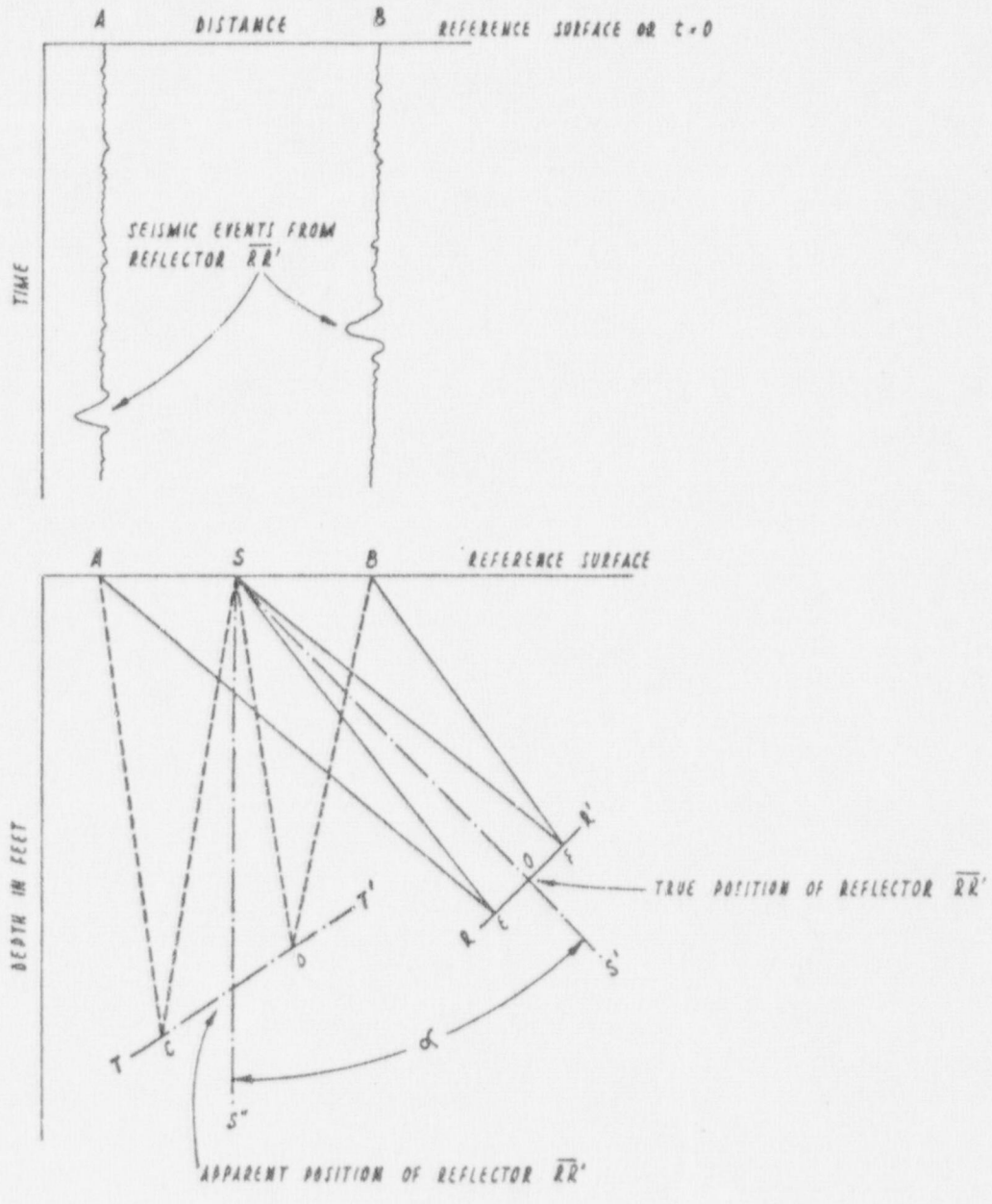

Figure 5. Geophones located at A and B record a seismic signal originating at S, and reflected from $\overline{RR'}$. If a constant velocity is assigned to the media through which the seismic waves travel, the distance may be calculated from the reference surface to the reflector. Lines $\overline{ACS}$ and $\overline{AES}$ are of equal length, as are Lines $\overline{SDB}$ and $\overline{SFB}$; therefore, the seismic travel times are identical for either path. Hence, unless the appropriate geometric corrections are made, reflector $\overline{RR'}$ will appear to be at position $\overline{TT'}$ on a seismic record section.

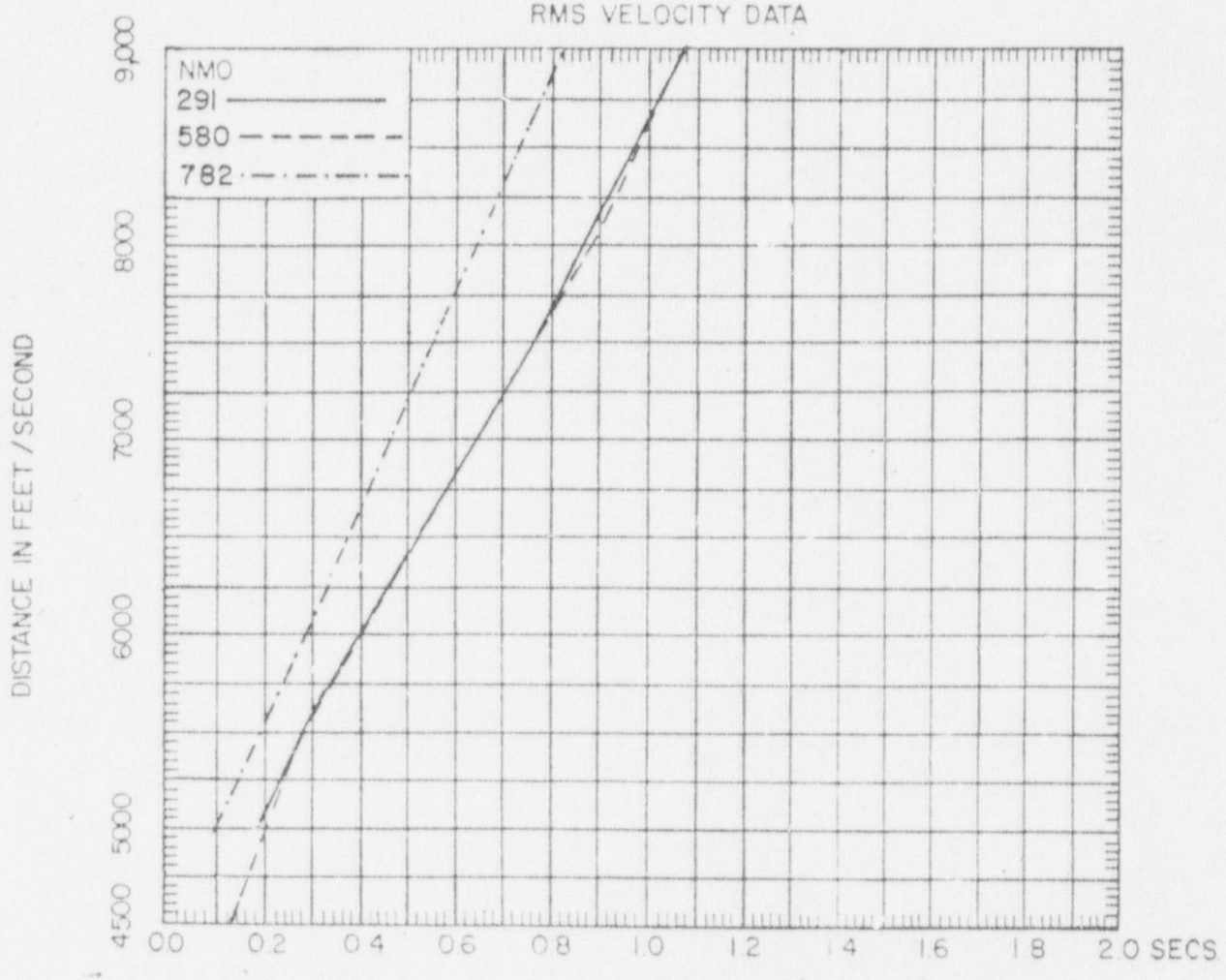

Figure 6. RMS velocity values determined by Aquatronics, Inc. for Line PB-4.

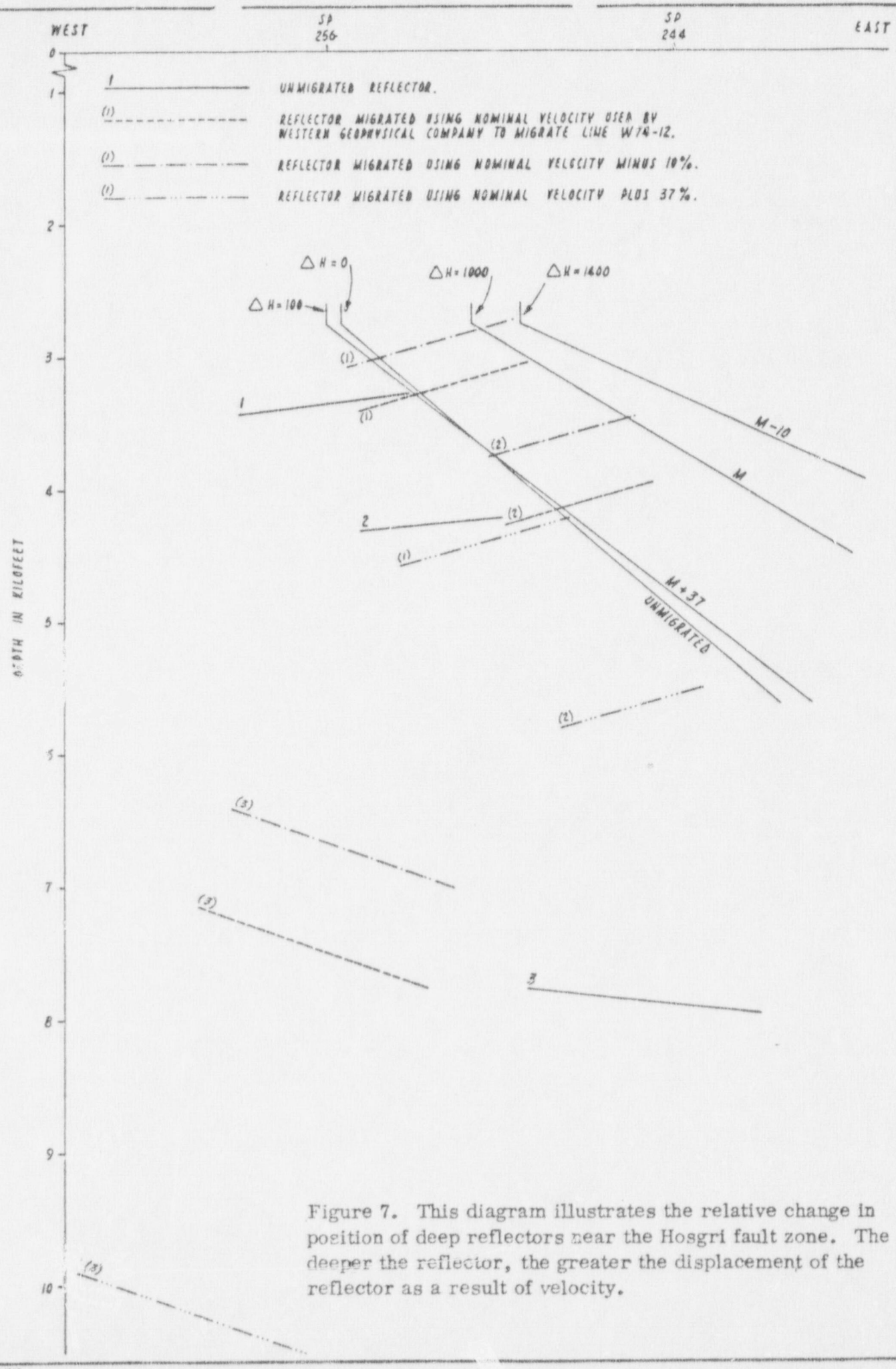

Figure 7. This diagram illustrates the relative change in position of deep reflectors near the Hosgri fault zone. The deeper the reflector, the greater the displacement of the reflector as a result of velocity.

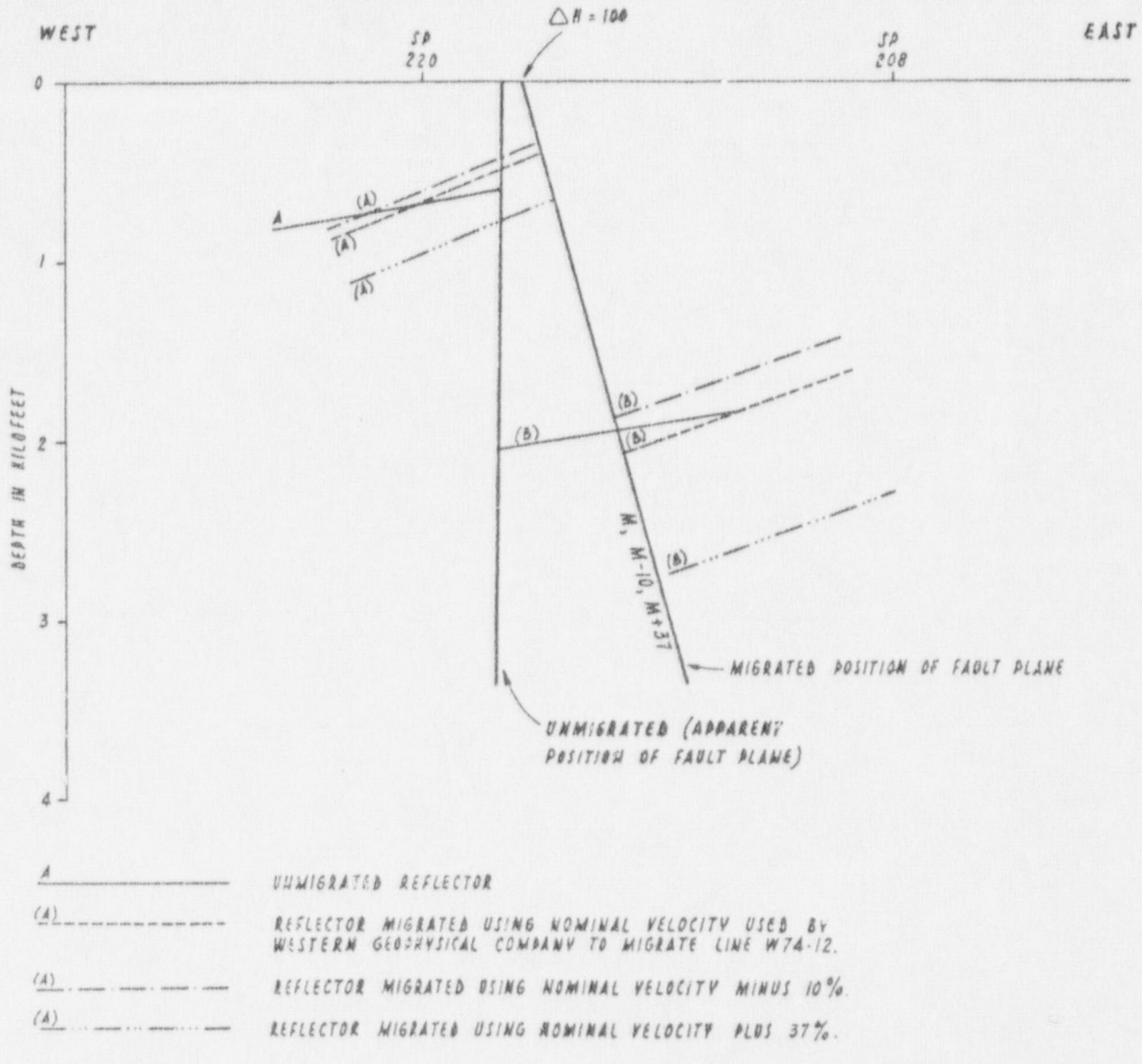

Figure 8. This diagram shows the relative change in position caused by velocity variation of two reflectors within the Hosgri fault zone. Since the reflectors are at a relatively shallow depth, the position of a fault structure based upon their location will not change greatly. Notice also that the steep dip of the fault causes position of the fault for each of the velocities used to be indistinguishably close to one another.